Croatian Society for Materials Protection

Metalurgija/Metallurgy

Vol. 65 No 1 / 2026

3D Roughness Parameters in Metal Surface Characterization

Andrej Razumić [1,*], Zvonko Trzun [1] and Zdenka Keran [2]

https://doi.org/10.64486/m.65.1.2

[1] Department of Polytechnics, Dr. Franjo Tuđman Defense and Security University, Ilica 256b, Zagreb, Croatia; zvonko.trzun@sois-ft.hr
[2] Faculty of Mechanical Engineering and Naval Architecture, University of Zagreb, Ivana Lučića 5, Zagreb, Croatia; zdenka.keran@fsb.unizg.hr
* Correspondence: andrej.razumic@sois-ft.hr

Type of the Paper: Review
Received: May 9, 2025
Accepted: August 12, 2025

Abstract: Surface characterization plays a crucial role in understanding the functional properties of metallic components, particularly in the context of advanced manufacturing technologies such as additive manufacturing and powder metallurgy. 3D roughness parameters, also called areal topography parameters, deliver a richer and more detailed characterization of surface features than conventional 2D approaches, offering insights into roughness, waviness, and other irregularities that influence the mechanical and functional performance of materials. This paper explores the application of areal topography parameters in characterizing metallic surfaces produced through various processing techniques, with a particular focus on laser surface treatment, powder compaction, and additive manufacturing. The study highlights the importance of selecting appropriate parameters to ensure reliable assessment of surface integrity, as well as their potential use in optimizing manufacturing processes. Special attention is given to the challenges associated with the standardization and interpretation of 3D parameters in industrial applications.

Keywords: surface topography; areal topography parameters; 3D topography parameters; surface characterization

1. Introduction

Unlike conventional two-dimensional (2D) profile metrics, which often fall short in capturing the complexity of surface morphology, three-dimensional roughness parameters, often called areal topography parameters, offer a more comprehensive insight into both the geometric configuration and functional behavior of surfaces [1]. Accurately describing surface topography through such parameters is essential for linking manufacturing techniques with the surface characteristics they produce [2].

To accurately describe the surface, there are a large number of areal topography parameters that describe the state of the measured area. Surface topography is measured by 2D and 3D techniques, resulting in line or areal topography parameters. Topography parameters are unfiltered and include deviation from shape, waviness, and roughness. When applying the 2D measurement method, by filtering with a standardized cut-off, the parameters of roughness *R* and waviness *W* are obtained. The parameters on the unfiltered profile are the primary parameters and are marked *P*. Usually, the parameters which describe the surface condition and are obtained by the 3D technique, are not filtered because there are no recommendations on whether and which cut-off values to use [3]. The obtained unfiltered parameters, commonly referred to by authors as areal topography

parameters, areal roughness parameters or 3D roughness parameters [4]. Inconsistent or insufficiently standardized terminology may lead to misinterpretation of measurement outcomes, underscoring the importance of harmonized definitions. Various surface topography parameters have been developed to systematically describe surface condition.

Areal topography parameters have significant applications across various aspects of metallurgy, particularly in evaluating surface integrity, wear resistance, and overall performance of machined components [5]. The application of surface topography parameters in the characterization of metallic surfaces represents an evolving field with significant implications for manufacturing, materials science, and engineering [6]. Surface integrity, which includes both the microstructural state and surface texture, is a key factor in applications demanding high performance in terms of wear resistance, corrosion prevention, and adhesive properties. Defects on the surface can serve as focal points for mechanical failure, making topographical analysis especially important [7]. Within this framework, 3D surface data has emerged as a critical element in optimizing manufacturing strategies and ensuring product quality across various industries [8], [9].

To evaluate how processing conditions influence surface behavior, a quantitative approach using three-dimensional topography parameters is indispensable [10], [11]. These parameters are especially valuable in assessing surface quality in both subtractive methods, such as machining, and additive manufacturing (AM) processes [12]. Their effectiveness in improving the structural performance of AM components has been well-documented. Furthermore, surface morphology holds a central role in powder metallurgy, where it affects both mechanical properties and process efficiency [13], [14].

In metallurgical contexts, surface analysis often depends on areal parameters due to their ability to describe both micro-roughness and macro-scale waviness. For example, presented a method using coherence scanning interferometry (CSI) to precisely evaluate the complex surface geometries of metal parts produced by AM techniques. Areal topography parameters can also be obtained using atomic force microscopy (AFM), which is now widely applied across numerous scientific and industrial fields [15]. AFM is particularly advantageous for its high spatial resolution, enabling the quantification of nanometer-scale roughness features that are not accessible with optical techniques. Furthermore, AFM-derived 3D parameters facilitate the correlation between nanoscale morphology and macroscopic material behavior, such as adhesion, wear resistance, and coating performance, making it a powerful tool for linking surface texture to functional properties [16].

Areal topography parameters are particularly useful for metals produced by additive manufacturing methods such as selective laser melting (SLM) and laser powder bed fusion (LPBF) [17]. These descriptors capture complex morphologies and reveal correlations with process variables like laser orientation and energy input [18]. Since surface texture governs properties such as friction, wear resistance, and fatigue, its characterization is essential for predicting component performance and lifetime [19], [20]. Within metallurgy, integrating surface analysis into processes such as cleaning, coating, and surface treatment provides a comprehensive approach to improving durability and functional efficiency [21]. As metallurgical techniques evolve alongside technological advancements, the role of surface topography will become increasingly prominent, aligning surface characteristics with desired functional properties [22], [23].

In addition to improving performance assessment, topography parameters play an increasingly important role in risk evaluation and failure prediction [24], [25]. By quantifying features such as peak distribution, valley depth, and surface anisotropy, they enable the identification of critical zones where stresses or corrosion processes may initiate [26]. Such analyses not only guide the design of more reliable components but also support risk-based maintenance strategies, reducing unexpected failures and extending service life [27].

2. List of areal topography parameters

The state of a surface can be described using a wide range of areal topography parameters, which are conventionally grouped into amplitude, spatial, hybrid, functional, and miscellaneous categories [28]. An overview of the principal 3D roughness parameters is provided in Table 1. The majority of these descriptors are standardized in the ISO 25178-2:2021 standard, *Geometrical Product Specifications (GPS) – Surface Texture: Areal – Part 2: Terms, Definitions, and Surface Texture Parameters* [28].

https://doi.org/10.64486/m.65.1.2

Table 1. List of areal topography parameters [29]

Symbol	Parameter	Category
Sa	Average Roughness	Height
Sku	Kurtosis	
Sp	Maximum Peak Height	
Sq	Root Mean Square Roughness	
Ssk	Skewness	
Sv	Maximum Valley Depth	
Sz	Maximum Height of Surface	
Sal	Autocorrelation Length	Spatial
Str	Texture Aspect Ratio	
Sdq	Root Mean Square (RMS) Surface Slope	Hybrid
Sdr	Developed Interfacial Area Ratio	
Sds	Summit Density	
Ssc	Mean Summit Curvature	
Sdc(mr)	Inverse Areal Material Ratio	
Sk	Core Roughness Depth	
Smr(c)	Areal Material Ratio	
Spk	Reduced Peak Height	
Svk	Reduced Valley Depth	
Sxp (p,q)	Peak Extreme Height	
Vm(mr)	Material Volume	
Vmc(p,q)	Core Material Volume	
Vmp(p)	Peak Material Volume	
Vv(mr)	Void Volume	
Vvc(p,q)	Core Void Volume	
Vvv(p)	Dale Void Volume	
Std	Texture Direction	Miscellaneous

In surface topography analysis, measurement results often include only the parameters *Ra* and *Rz*, or *Sa* and *Sz*. This limited reporting can lead to misinterpretation of the surface characteristics of the analyzed sample. To obtain reliable quantitative assessments of surface topography, it is essential to understand which parameters should be monitored and how they should be interpreted. This paper provides an overview of surface topography parameters, including their definitions, explanations, and representative examples.

3. Application of areal topography parameters

Since surface condition is difficult to describe using a single parameter, a wide range of areal parameters has been developed. The application of selected parameters is described below.

https://doi.org/10.64486/m.65.1.2

3.1. Amplitude parameters

According to the ISO 25178-2:2021 standard, Geometrical product specifications (GPS) – Surface texture: Areal – Part 2: Terms, definitions and surface texture parameter [28], amplitude areal topography parameters include the following:

- *Sa* – Arithmetical mean height of the scale-limited surface. This is the most commonly used parameter, representing the arithmetic mean of the absolute deviations of surface heights from the mean plane. It is defined by the following mathematical expression:

$$Sa = \sqrt{\frac{1}{A}\iint_A |z(x,y)|dxdy} \tag{1}$$

- *Sq* – Root mean square height of the scale-limited surface. This parameter is defined as:

$$Sq = \sqrt{\frac{1}{A}\iint_A z^2(x,y)dxdy} \tag{2}$$

- *Ssk* – Skewness of the scale-limited surface. A value of *Ssk* = 0 indicates a symmetric (normally distributed) height distribution. A positive *Ssk* value suggests that the majority of the deviations lie below the mean plane (i.e., dominated by peaks), while a negative value implies that the deviations are primarily above the mean (i.e., dominated by pits).

$$Ssk = \frac{1}{Sq^3}\left[\frac{1}{A}\iint_A z^3(x,y)dxdy\right] \tag{3}$$

- *Sku* – Kurtosis of the scale-limited surface. This parameter characterizes the sharpness of surface features by describing the concentration of peaks and valleys. It is useful for evaluating the contact behavior between surfaces and is sometimes referred to as a measure of surface sharpness.

$$Sku = \frac{1}{Sq^4}\left[\frac{1}{A}\iint_A z^4(x,y)\,dxdy\right] \tag{4}$$

- *Sp* – Maximum peak height of the scale limited surface.
- *Sv* – Maximum pit height of the scale limited surface.
- *Sz* – Maximum height of the scale-limited surface.

$$Sz = Sp + Sv \tag{5}$$

In three-dimensional surface characterization, the most commonly employed height-based parameters are *Sa* (arithmetical mean height) and *Sq* (root mean square height). These parameters provide a global indication of the average roughness level by quantifying height deviations with respect to the mean reference plane [30], [31]. *Sa* is defined as the arithmetic average of the absolute height values, whereas *Sq* is calculated as the root mean square of the same deviations. Although both parameters are simple to interpret and widely used, they are limited in their ability to capture surface morphology in detail [32]. In particular, these parameters are unable to differentiate between elevations and depressions, nor do they capture how surface features are distributed laterally [33]. As a result, surfaces with markedly different morphologies may yield the same *Sa* and *Sq* values, limiting their reliability when applied in isolation. Nevertheless, in cases where the surface characteristics or intended functional role are well established, these parameters remain valuable for detecting significant

https://doi.org/10.64486/m.65.1.2

deviations in processing quality or material performance. [33]. In applied research, *Sq* is frequently used in the characterization of optical surfaces [31], additively manufactured metals [34], [35], and biomaterials such as dental cements and composite restoratives [36], while *Sa* is traditionally applied in the evaluation of machined and engineered surfaces [37].

For surfaces following a Gaussian distribution, the skewness parameter (*Ssk*) equals zero and the kurtosis parameter (*Sku*) equals three. These descriptors provide complementary information that cannot be obtained from *Sa* or *Sq* alone. *Ssk* is particularly effective in monitoring wear processes, honing, and porosity development, as it describes the asymmetry of the height distribution [38], [39]. *Sku*, on the other hand, is sensitive to extreme deviations such as isolated peaks or deep pits, making it suitable for detecting surface defects and irregularities in critical components [40], [41]. Because both parameters are derived from higher-order statistical moments, reliable characterization requires an adequate sampling density and the application of filtering procedures to eliminate measurement artefacts [36], [42]. Compared to *Sa* and *Sq*, *Ssk* and *Sku* enable a more refined interpretation of surface topography, particularly in cases where functional performance depends on the presence of sharp asperities, load-bearing capacity, or surface porosity [43].

Parameters based on extreme points of the surface, such as *Sp* (maximum peak height), *Sv* (maximum pit depth), and *Sz* (maximum height difference), provide additional insights into functional performance [44]. However, as they are defined by single data points, their repeatability may be limited [45], [15]. Careful selection of cut-off and filtering conditions is therefore necessary to minimize the influence of anomalous features [46]. Among these, *Sz* is particularly relevant in applications involving coatings, sealing, and lubrication, as it reflects the overall vertical range of the surface and strongly correlates with fluid retention capability. In comparison with *Sa* and *Sq*, these parameters offer localized information on surface extremes rather than global averages, which is advantageous when evaluating functional failures caused by deep scratches, coating defects, or sharp protrusions.

In the context of metal surface characterization, these parameters play complementary roles. *Sa* and *Sq* are particularly valuable for monitoring machining quality, polishing efficiency, and deviations introduced during finishing operations. *Ssk* and *Sku* provide essential insights into wear progression, fatigue initiation, and the development of pores or cracks in metallic substrates, making them critical for the evaluation of load-bearing components and tribological interfaces [34], [38]. Finally, *Sz* and related extreme-value parameters are frequently employed to assess coatings on metallic surfaces, where peak and valley distribution governs adhesion, sealing efficiency, and lubrication retention. Together, these parameters establish a multi-level framework that connects global roughness assessment with localized and functional descriptors, enabling a more comprehensive understanding of the relationship between surface morphology and performance in metallic systems.

To rigorously illustrate these relationships, visual representation of surface topography is essential. Figure 1 demonstrates that two surfaces may yield identical values of the amplitude parameters (*Sa*, *Sq*, *Ssk*, *Sku*, *Sp*, *Sv*, *Sz*), as summarized in Table 2, while exhibiting distinctly different morphological features.

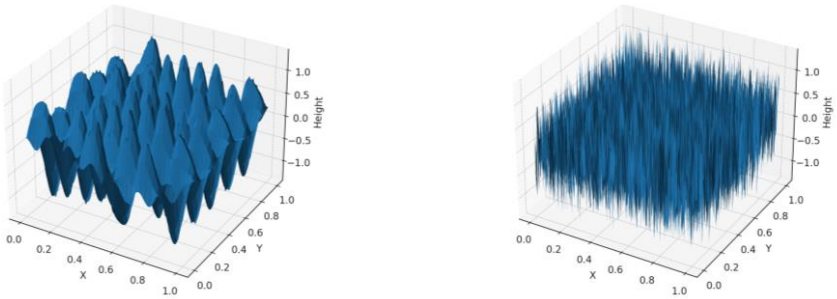

a) periodic surface b) randomized surface

Figure 1. Different surfaces with the same height parameters

https://doi.org/10.64486/m.65.1.2

Table 2. Height-based roughness parameters the surfaces shown in Figure 1

Parameter	***Sa*/μm**	***Sq*/μm**	***Ssk*/–**	***Sku*/–**	***Sp*/μm**	***Sv*/μm**	***Sz*/μm**
Surface A	0.432723	0.530905	–0.002949	2.424498	1.386362	1.387198	2.77356
Surface B	0.432723	0.530905	–0.002949	2.424498	1.386362	1.387198	2.77356

This observation underscores the inherent limitations of relying solely on conventional height areal parameters. Accordingly, a comprehensive surface characterization requires the inclusion of complementary parameters capable of capturing spatial organization, functional performance, and material ratio properties, as elaborated in the subsequent sections.

3.2. Spatial parameters

In addition to height areal parameters, spatial parameters provide essential insight into the lateral organization of surface features. Among them, the texture aspect ratio (*Str*) and the autocorrelation length (*Sal*) are widely used to characterize isotropy and spatial correlation in surface morphology. With the advancement of technology and informatics, the development of the Autocorrelation Function (ACF) has enabled the calculation and visualization of spatial parameters. Spatial autocorrelation describes the degree of similarity between surface features over a given area. It assesses whether observed data points are spatially interrelated and can be classified as either positive or negative. All spatial parameters are defined based on the texture of the observed surface.

- *Sal* – Auto-Correlation Length. It represents the horizontal distance in the direction in which the autocorrelation function decays the fastest.

$$Sal = \min_{t_x,t_y \in R} \sqrt{t_x^2 + t_y^2} \tag{6}$$

where is

$$R = \{(t_x, t_y): f_{ACF}(t_x, t_y) \leq s\} \tag{7}$$

- *Str* – Texture Aspect Ratio. The parameter describes the uniformity of the surface texture by evaluating anisotropy. It is calculated as the ratio between the shortest and longest autocorrelation lengths, i.e., the distances in the directions where the autocorrelation function decays the fastest and slowest, respectively. This parameter is particularly useful for determining the predominant orientation of surface features. Str tends toward zero for highly directional textures, and approaches one for isotropic surfaces where no dominant orientation is observed. It is mathematically defined as:

$$Str = \frac{\min\limits_{t_x,t_y \in R} \sqrt{t_x^2 + t_y^2}}{\max\limits_{t_x,ty \in Q} \sqrt{t_x^2 + ty^2}} \tag{8}$$

where is

$$R = \{(t_x, t_y): f_{ACF}(t_x, t_y) \leq s\}, Q = \{(t_x, t_y): f_{ACF}(t_x, t_y) \geq s\} \tag{9}$$

The *Str* parameter quantifies the degree of directional uniformity in a surface texture. Values close to one indicate isotropic surfaces, whereas low values highlight pronounced anisotropy, typically associated with machining operations such as grinding, milling, or turning. In metallic surfaces, *Str* is frequently employed to evaluate lay patterns resulting from multi-pass processing and to detect secondary orientations caused by vibration of machine tools [47]. A limitation of *Str*, however, is its sensitivity to complex textures that contain multiple directional components, where interpretation may become ambiguous and strongly dependent on filtering strategies [48].

https://doi.org/10.64486/m.65.1.2

The *Sal* parameter represents the characteristic distance over which height data remain statistically correlated. In practical terms, it indicates the spacing at which surface features lose their similarity, making it an important criterion for defining sampling intervals in measurement strategies. In tribological studies of metallic components, *Sal* has been linked to frictional response and wear evolution, where the lateral spacing of asperities directly affects the formation of contact junctions. It is also applied in assessing ground and polished steels, where *Sal* provides insight into the regularity of grooves and their influence on lubrication. One drawback of *Sal* is that its value can vary substantially depending on measurement resolution and the method used to compute the autocorrelation function, which may complicate direct comparisons between studies.

To illustrate the relevance of these parameters, visual representation of the autocorrelation function is particularly informative. Such plots reveal the spatial decay of correlation, allowing *Sal* to be identified at the point where correlation diminishes to a threshold, and the isotropy of the function's contour to be used in deriving *Str* [49]. These visual tools complement the numerical descriptors, enabling clearer interpretation of spatial organization in metallic surfaces, particularly when global height parameters alone fail to distinguish between morphologically different textures.

3.3. Hybrid parameters

Hybrid surface parameters combine both amplitude and spatial information, offering a more comprehensive description of topography than height descriptors alone [31]. They are particularly relevant when surfaces with similar average roughness values exhibit markedly different functional performance due to differences in slope, complexity, or material-bearing capacity. Hybrid parameters describe variations in surface texture that result from a combination of amplitude and spatial characteristics.

- *Sdq* – Root Mean Square (RMS) Surface Slope. *Sdq* quantifies the average slope of the surface texture. A surface with steeper slopes will have a higher *Sdq* value, whereas a smoother surface with gradual transitions will have an *Sdq* value approaching zero.

$$Sdq = \sqrt{\frac{1}{A}\iint_A \left[\left(\frac{\partial z(x,y)}{\partial x}\right)^2 + \left(\frac{\partial z(x,y)}{\partial y}\right)^2\right] dxdy} \tag{10}$$

The root mean square gradient (*Sdq*) measures surface steepness, integrating both vertical variation and lateral feature density. It differentiates between surfaces of identical Sa but varying spacing—sharp vs. broad asperities—and is critical in assessing sealing interfaces, optics, and coatings [50], [51]. However, *Sdq* is highly sensitive to resolution and filtering protocols, potentially limiting comparability. As illustrated in Figure 2, two surfaces can exhibit nearly identical *Sa* values while differing significantly in *Sdq*, highlighting the importance of slope-based descriptors for distinguishing surface morphology.

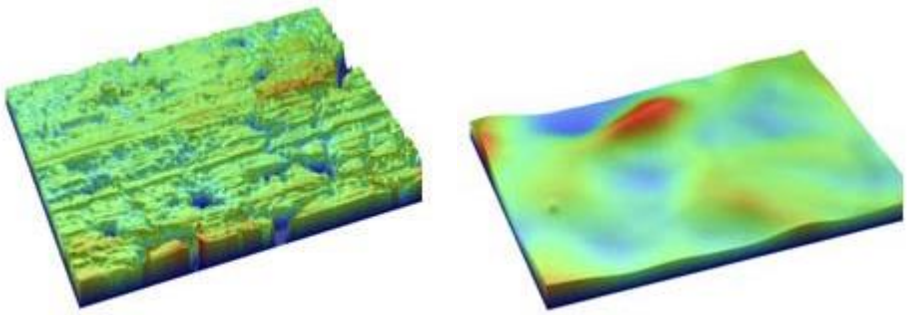

Figure 2. Surfaces with nearly identical *Sa* values but different *Sdq* parameters [52]
Sa = 80 nm, *Sdq* = 11,0 *Sa* = 75 mm, *Sdq* = 0,2

https://doi.org/10.64486/m.65.1.2

- *Sdr* – Developed Interfacial Area Ratio. The ratio of the increment of surface diversity in the observed area. It is expressed as the percentage of the area that deviates from the ideal plane. The amount of the parameter increases if the observed surface has sudden changes in slope.

The developed interfacial area ratio (*Sdr*) expresses the increase in actual surface area relative to its projected baseline, growing as surface texture complexity increases (finer features, steeper slopes) even when *Sa* remains fixed. *Sdr* is vital in adhesion, coating, and tribological contexts [53]. Yet, highly stochastic textures can yield similar *Sdr* values despite different morphologies, making interpretation scale-dependent [54].

3.4. Functional parameters

Functional parameters translate surface topography into performance-relevant characteristics by assessing how surface geometry relates to mechanical function. Rather than focusing solely on height or spatial variation, these parameters derive from the material ratio curve – a representation of how material accumulates from the peaks down to the valleys. They enable the quantification of load-bearing capacity, lubrication retention, sealing behavior, and wear susceptibility, making them essential in engineering applications [55]. This is especially critical in metallic components where tribological performance is governed by the interaction between surface geometry and contact mechanics [56], [57]. However, because functional parameters depend on defined reference depths, material ratio thresholds, and measurement strategies, consistent interpretation requires standardized measurement protocols to ensure reproducibility and comparability [58].

- *Smr(c)* – Areal Material Ratio. This parameter represents the ratio of material within a given height (*c*) over the surface area in the observed spatial plane. It is often expressed as a percentage and relates to the cumulative probability function of the ordinate. Figure 3 illustrates the material ratio on the observed surface.

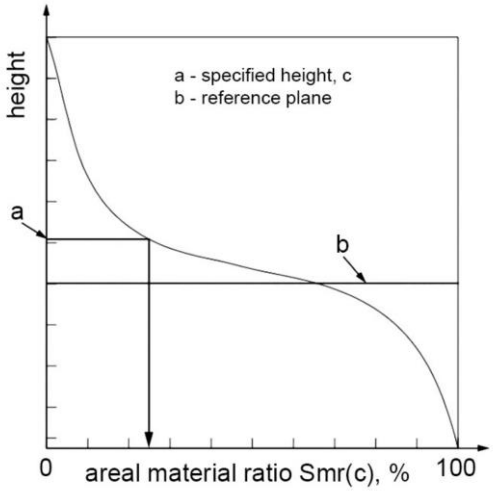

Figure 3. Material ratio curve of the analyzed surface [28]

The material ratio at a specified depth (*Smr(c)*) provides insight into the functional load-bearing capacity of a surface by quantifying the fraction of material remaining at a defined depth [59]. A well-known application is the specification of cylinder liner surfaces in combustion engines. Plateau-honed surfaces, for example, are engineered to maximize *Smr(c)* values at operational depths, thereby ensuring sufficient support for piston rings while retaining pockets for lubricant storage. Still, *Smr(c)* is highly dependent on the chosen reference depth and material ratio, which means that small changes in definition can significantly alter the reported values.

- *Vm(mr)* – the Void Volume. This parameter refers to the volume of material covering the surface, from a height corresponding to a selected value of mr, up to the highest peak of the surface [48] The value of mr can range from 0 % to 100 %.

https://doi.org/10.64486/m.65.1.2

- *Vmp(p)* – Dale Void Volume. *Vmp* represents the volume of material in the ratio of surface area determined by a specified percentage (p%). The default values for p% are specified in ISO 25178-3 [60].
- *Vmc* - Core Void Volume. The Core Void Volume represents the difference in volume between two material ratios, q% and p%, as defined in ISO 25178-3 [60]. The mathematical notation is as follows:

$$Vmc = Vm(q) - Vm(p) \tag{11}$$

Functional parameters extend this analysis by capturing how much material or void space is present within defined regions of the surface. The peak material volume (*Vmp*) estimates the amount of material in the highest surface layers, which is critical for sealing performance and the initial stages of wear [61]. The core material volume (*Vmc*) quantifies the load-bearing portion of the surface after the uppermost asperities have been removed, providing an indication of long-term durability. These parameters are employed in sealing applications, where *Vmp(p)* indicates the volume of material contributing to effective sealing performance [61].

- *Vv(mr)* – Void Volume. *Vv* refers to the volume of space between the surface structure, extending from a height corresponding to the selected value of *mr* down to the lowest valley. The value of *mr* can range from 0% to 100%.

$$Vv(p) = \frac{K}{100\%} \int_{0}^{100} [S_{mc}(p) - S_{mc}(q)]\, dq \tag{12}$$

- *Vvv(p)* – Dale Void Volume. This parameter quantifies the volume at a given p% of material. The default p% value is 80%, though other values specified by ISO 25178-3 [60] can be used.
- *Vvc(p,q)* – Core Void Volume. *Vvc* represents the volume of core voids in the surface, defined by the difference between the void volumes at p% and q% material ratios. The default values for p% and q% are specified in ISO 25178-3 [60].

Complementary void-related parameters such as valley void volume (*Vvv*) and core void volume (*Vvc*) describe the storage capacity of valleys and the residual space within the surface core. These descriptors are essential for predicting lubrication retention, debris entrapment, and the performance of coatings in metallic systems [62]. Similar to *Smr(c)*, these values are sensitive to the selection of cut-off levels and material ratio thresholds, which can make cross-study comparisons challenging [63].

By integrating slope, surface enlargement, material ratio, and volumetric aspects, hybrid parameters link purely geometrical descriptors to functional performance. Their relevance is evident in tribology, sealing technologies, and surface engineering of metals, where hybrid characteristics govern not only contact mechanics but also lubrication efficiency and coating integrity. Nonetheless, their sensitivity to measurement conditions, filtering strategies, and reference definitions highlights the importance of standardized approaches and careful interpretation.

3.5. Miscellaneous parameters

The texture direction parameter (*Std*) quantifies the angular orientation of the dominant lay of a surface with respect to the y-axis, where alignment along the y-axis corresponds to *Std* = 0°. Although this descriptor is not formally standardized in ISO 25178-2 [28], it provides valuable insights into anisotropic surface features that directly affect functional performance. For example, in sealing applications, even small deviations in texture orientation can alter the distribution of contact stresses, leading to leakage or accelerated wear. Similarly, in tribological systems such as sliding bearings or piston-cylinder assemblies, directional texture can influence frictional behavior, fluid entrainment, and wear mechanisms. Figure 4 illustrates how the texture direction (*Std*) quantifies the prevailing orientation of surface features relative to the reference axis, providing complementary insight into surface anisotropy.

https://doi.org/10.64486/m.65.1.2

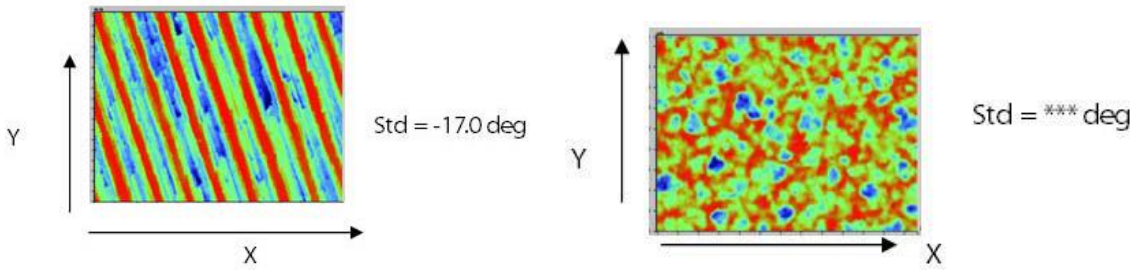

Figure 4. Texture direction (*Std*) of the analyzed surface [29]

One advantage of *Std* is its ability to detect remnants of preliminary machining processes, such as turning or milling, that may persist after subsequent finishing operations like grinding or polishing [64]. For instance, a surface exhibiting *Std* ≈ 0° may correspond to a strongly directional lay produced by turning, whereas a more isotropic finish generated by lapping could yield Std values that fluctuate around random orientations. By providing such directional information, Std complements the texture aspect ratio (*Str*), which measures the degree of isotropy in a surface. While *Str* indicates how uniformly features are distributed, Std specifies the prevailing orientation. Together, these parameters allow a more comprehensive description of anisotropic topographies.

Despite its utility, several limitations of *Std* must be considered. First, the parameter is highly sensitive to measurement strategy, particularly the filtering method, scan size, and resolution, which can introduce artefacts or bias [65]. Second, surfaces with multiple texture orientations may yield ambiguous Std values, as the method typically assigns only one dominant direction. Third, the absence of standardization reduces comparability across studies, highlighting the need for harmonized protocols [66]. Quantitative case studies, such as the difference between *Std* ≈ 0° for turned surfaces and *Std* ≈ 45° for cross-hatched honing patterns, further demonstrate its discriminative power, but also reveal that its interpretation requires contextualization within the broader set of surface descriptors. By explicitly addressing directional properties, *Std* enriches the analysis of engineered surfaces, especially when combined with isotropy descriptors like *Str*. Its effective use, however, depends on careful measurement design, critical interpretation of results, and an awareness of its methodological constraints.

4. Conclusion

This study provides a comprehensive overview of the application of areal surface topography parameters in the characterization of metallic surfaces. Compared to conventional profile (line) parameters, areal parameters offer a significantly more detailed and representative depiction of surface morphology, capturing spatial complexity and functional attributes that are often overlooked by linear measurements. Although profile parameters still predominate in industrial and academic settings, recent technological advancements and evolving application requirements are driving a shift toward broader adoption of areal surface characterization methods.

Despite their clear advantages, areal parameters should not be viewed as a replacement for profile measurements, but rather as a complementary approach. A frequent shortcoming in current practice is the predominant use of basic parameters such as *Sa* and *Sz*. While these provide a general indication of surface roughness, their isolated use may lead to misleading or incomplete interpretations, particularly when functional performance is critical.

Effective surface characterization requires selecting parameter sets tailored to the specific function and context of the surface. For example, within metal additive manufacturing techniques including selective laser melting and powder bed fusion, parameters including *Sa*, *Sq*, *Sdr*, *Spk*, and *Svk* are essential for quality control and performance prediction. In applications involving sealing and tribological performance, parameters such as *Smr(c)*, *Vm*, *Vvv*, and *Std*, along with volume-based metrics like *Vmp* and *Vvc*, provide valuable insight into lubricant retention and sealing capability. In serial production environments, although reliance on *Sa* and *Sz* is

https://doi.org/10.64486/m.65.1.2

common, incorporating function-specific parameters such as *Sdq* (for optical components) or *Ssk* and *Sku* (for wear-prone elements) can significantly enhance the reliability of surface assessments. Furthermore, in the development of surface treatments and coatings, a combination of amplitude (*Sa*, *Sdq*), spatial (*Str*), and functional parameters (*Sdr*, *Vm*, *Vvc*) enables more accurate tracking of surface evolution and process optimization. Areal parameters are also increasingly employed as input data for contact mechanics, tribological, and thermal simulations, where metrics such as Str and Sal are particularly beneficial for modeling anisotropic or textured surfaces.

To ensure consistent and meaningful application of areal topography parameters, it is recommended to adopt ISO 25178 standards within quality management systems and to provide adequate training for technical personnel in parameter selection and interpretation. In collaborative environments, especially those involving external suppliers or research partners, clearly specifying relevant parameters and their functional justification enhances the reliability, reproducibility, and comparability of surface measurements.

Ultimately, the application of areal surface topography parameters, when guided by functional relevance and implemented within a standardized framework, substantially improves the fidelity of surface characterization. This contributes not only to enhanced quality control and product performance but also to the advancement of research and development in surface engineering.

References

[1] B. He, D. P. Webb, and J. Petzing, 'Areal Surface Texture Parameters for Copper/Glass Plating Adhesion Characteristics', *Measurement Science Review*, vol. 21, no. 1, pp. 11–18, Feb. 2021, https://doi.org/10.2478/msr-2021-0002

[2] A. Bazan, P. Turek, P. Sułkowicz, Ł. Przeszłowski, and A. Zakręcki, 'Influence of the Size of Measurement Area Determined by Smooth-Rough Crossover Scale and Mean Profile Element Spacing on Topography Parameters of Samples Produced with Additive Methods', *Machines*, vol. 11, no. 6, p. 615, 2023, https://doi.org/10.3390/machines11060615

[3] A. Razumić *et al.*, 'Atomic Force Microscopy: Step Height Measurement Uncertainty Evaluation', *Tehnički glasnik*, vol. 18, no. 2, pp. 209–214, May 2024, https://doi.org/10.31803/tg-20230829155921

[4] A. Razumić, 'Procjena mjerne nesigurnosti rezultata mjerenja na području mikroskopije atomskih sila u dimenzijskom nanomjeriteljstvu', Ph.D. Thesis, University of Zagreb, Faculty of Mechanical Engineering and Naval Architecture, 2024. Accessed: May 13, 2024. [Online]. Available: https://urn.nsk.hr/urn:nbn:hr:235:432266

[5] E.-P. Heikkinen, T. Fabritius, and J. Riipi, 'Holistic Analysis on the Concept of Process Metallurgy and Its Application on the Modeling of the AOD Process', *Metall Mater Trans B*, vol. 41, no. 4, pp. 758–766, Aug. 2010, https://doi.org/10.1007/s11663-010-9368-2

[6] M. Shaat, 'Effects of surface integrity on the mechanics of ultra-thin films', *International Journal of Solids and Structures*, vol. 136–137, pp. 259–270, Apr. 2018, https://doi.org/10.1016/j.ijsolstr.2017.12.019

[7] S. Bhattacharya, R. Sahara, D. Božić, and J. Ruzic, 'Data analytics approach to predict the hardness of copper matrix composites', *Metallurgical and Materials Engineering*, vol. 26, Nov. 2020, https://doi.org/10.30544/567

[8] N. Senin, A. Thompson, and R. K. Leach, 'Characterisation of the topography of metal additive surface features with different measurement technologies', *Meas. Sci. Technol.*, vol. 28, no. 9, p. 095003, Sep. 2017, https://doi.org/10.1088/1361-6501/aa7ce2

[9] N. Senin, A. Thompson, and R. Leach, 'Feature-based characterisation of signature topography in laser powder bed fusion of metals', *Meas. Sci. Technol.*, vol. 29, no. 4, p. 045009, Apr. 2018, https://doi.org/10.1088/1361-6501/aa9e19

[10] V. Molnar, 'Influence of cutting parameters and tool geometry on topography of hard turned surfaces', *Machines*, vol. 11, no. 6, p. 665, 2023, https://doi.org/10.3390/machines11060665

[11] J. Das and B. Linke, 'Evaluation and systematic selection of significant multi-scale surface roughness parameters (SRPs) as process monitoring index', *Journal of Materials Processing Technology*, vol. 244, pp. 157–165, 2017, https://doi.org/10.1016/j.jmatprotec.2017.01.017

[12] J. Lee, M. S. Hossain, M. Taheri, A. Jameel, M. Lakshmipathy, and H. Taheri, 'Characterization of surface topography features for the effect of process parameters and their correlation to quality monitoring in metal additive manufacturing', *Metrology*, vol. 2, no. 1, pp. 73–83, 2022, https://doi.org/10.3390/metrology2010005

https://doi.org/10.64486/m.65.1.2

[13] Z. Yan, D. Yin, L. Luo, G. He, and Z. Dai, 'Integrated product and process development of powder metallurgy hub for automotive clutch', *Powder Metallurgy*, vol. 62, no. 4, pp. 247–257, Aug. 2019, https://doi.org/10.1080/00325899.2019.1639917

[14] A. M. Abraham and S. Venkatesan, 'A critical review on biomaterials using powder metallurgy method', *Engineering Research Express*, vol. 6, no. 1, p. 012508, 2024, https://doi.org/10.1088/2631-8695/ad35a6

[15] A. Razumić *et al.*, 'Atomic force microscope: measurement uncertainty evaluation of 3D topography parameters', in *MATRIB 2024-International conference on Materials, Tribology, Recycling*, 2024, pp. 318–329.

[16] A. Razumić, A. Horvatić Novak, B. Štrbac, and B. Runje, 'Influence of scan parameters on surface topography obtained via AFM', in *International Scientific Conference (ETIKUM 2021)*, 2021, pp. 17–20.

[17] B. Raeymaekers and T. Berfield, 'Characterizing the as-built surface topography of Inconel 718 specimens as a function of laser powder bed fusion process parameters', *Rapid Prototyping Journal*, vol. 31, no. 1, pp. 200–217, 2025, https://doi.org/10.1108/RPJ-05-2024-0190

[18] S. R. Narasimharaju *et al.*, 'Surface texture characterization of metal selective laser melted part with varying surface inclinations', *Journal of Tribology*, vol. 143, no. 5, p. 051106, 2021, https://doi.org/10.1115/1.4050455

[19] G. P. Zhang, X. J. Liu, W. L. Lu, and X. Q. Jiang, 'Investigation of surface topography at the end of running-in process', *Applied Mechanics and Materials*, vol. 437, pp. 564–567, 2013, https://doi.org/10.4028/www.scientific.net/AMM.437.564.

[20] D. Zhu, L. Xu, F. Wang, T. Liu, and K. Lu, 'Evolution of metal surface topography during fatigue', *Metals*, vol. 7, no. 2, p. 66, 2017, https://doi.org/10.3390/met7020066

[21] L. Newton *et al.*, 'Optimisation of imaging confocal microscopy for topography measurements of metal additive surfaces', *Metrology*, vol. 3, no. 2, pp. 186–221, 2023, https://doi.org/10.3390/metrology3020011

[22] A. Biesiekierski, Y. Li, and C. Wen, 'The Application of the Rare Earths to Magnesium and Titanium Metallurgy in Australia', *Advanced Materials*, vol. 32, no. 18, p. 1901715, May 2020, https://doi.org/10.1002/adma.201901715

[23] Z. Keran, A. Horvatić Novak, A. Razumić, B. Runje, and P. Piljek, 'In-Crystal Dislocation Behaviour and Hardness Changes in the Case of Severe Plastic Deformation of Aluminium Samples', *Tehnički glasnik*, vol. 17, no. 2, pp. 231–236, 2023, https://doi.org/10.31803/tg-20230424191508

[24] D. Božić, B. Runje, and A. Razumić, 'Risk Assessment Procedure for Calibration', *Tehnički glasnik*, vol. 19, no. si1, pp. 7–12, 2025, https://doi.org/10.31803/tg-20250312153704

[25] D. Božić, B. Runje, and A. Razumić, 'Risk assessment for linear regression models in metrology', *Applied Sciences*, vol. 14, no. 6, p. 2605, 2024, https://doi.org/10.3390/app14062605

[26] Z. Keran, B. Runje, P. Piljek, and A. Razumić, 'Roboforming in ISF—Characteristics, Development, and the Step Towards Industry 5.0', *Sustainability*, vol. 17, no. 6, p. 2562, 2025, https://doi.org/10.3390/su17062562

[27] B. Runje, A. H. Novak, A. Razumić, P. Piljek, B. Štrbac, and M. Orosnjak, 'Evaluation of consumer and producer risk in conformity assessment decisions', in *30th Daaam International Symposium On Inteligent Manufacturing And Automation*, Danube Adria Association for Automation and Manufacturing, DAAAM, Vienna, 2019. https://doi.org/10.2507/30th.daaam.proceedings.007

[28] ISO 25178-2:2021 – Geometrical product specifications (GPS) – Surface texture: Areal – Part 2: Terms, definitions and surface texture parameter.

[29] 'Michigan Metrology - Surface Texture Parameters List by Name'. Accessed: May 30, 2022. [Online]. Available: https://www.michmet.com/texture_parameters_index_by_name.html

[30] A. Duparré, J. Ferre-Borrull, S. Gliech, G. Notni, J. Steinert, and J. M. Bennett, 'Surface characterization techniques for determining the root-mean-square roughness and power spectral densities of optical components', *Appl. Opt., AO*, vol. 41, no. 1, pp. 154–171, Jan. 2002, https://doi.org/10.1364/AO.41.000154

[31] P. Pawlus, R. Reizer, and M. Wieczorowski, 'Functional importance of surface texture parameters', *Materials*, vol. 14, no. 18, p. 5326, 2021, https://doi.org/10.3390/ma14185326

[32] S. Schröder, A. Duparré, L. Coriand, A. Tünnermann, D. H. Penalver, and J. E. Harvey, 'Modeling of light scattering in different regimes of surface roughness', *Optics express*, vol. 19, no. 10, pp. 9820–9835, 2011, https://doi.org/10.1364/OE.19.009820

[33] N. A. Feidenhans *et al.*, 'Comparison of optical methods for surface roughness characterization', *Measurement Science and Technology*, vol. 26, no. 8, p. 085208, 2015, https://doi.org/10.1088/0957-0233/26/8/085208

https://doi.org/10.64486/m.65.1.2

[34] S. Lee, B. Rasoolian, D. F. Silva, J. W. Pegues, and N. Shamsaei, 'Surface roughness parameter and modeling for fatigue behavior of additive manufactured parts: A non-destructive data-driven approach', *Additive Manufacturing*, vol. 46, p. 102094, 2021, https://doi.org/10.1016/j.addma.2021.102094

[35] A. Bhatt *et al.*, '*In situ* characterisation of surface roughness and its amplification during multilayer single-track laser powder bed fusion additive manufacturing', *Additive Manufacturing*, vol. 77, p. 103809, Sep. 2023, https://doi.org/10.1016/j.addma.2023.103809

[36] P. Zmarzły, T. Kozior, and D. Gogolewski, 'The effect of non-measured points on the accuracy of the surface topography assessment of elements 3D printed using selected additive technologies', *Materials*, vol. 16, no. 1, p. 460, 2023, https://doi.org/10.3390/ma16010460

[37] V. Alar, A. Razumić, B. Runje, I. Stojanović, M. Kurtela, and B. Štrbac, 'Application of Areal Topography Parameters in Surface Characterization', *Applied Sciences*, vol. 15, no. 12, p. 6573, 2025, https://doi.org/10.3390/app15126573

[38] N. Tayebi and A. A. Polycarpou, 'Modeling the effect of skewness and kurtosis on the static friction coefficient of rough surfaces', *Tribology international*, vol. 37, no. 6, pp. 491–505, 2004, https://doi.org/10.1016/j.triboint.2003.11.010

[39] M. Sedlaček, P. Gregorčič, and B. Podgornik, 'Use of the Roughness Parameters Ssk and Sku to Control Friction—A Method for Designing Surface Texturing', *Tribology Transactions*, vol. 60, no. 2, pp. 260–266, Mar. 2017, https://doi.org/10.1080/10402004.2016.1159358

[40] S.-C. Vladescu, A. V. Olver, I. G. Pegg, and T. Reddyhoff, 'The effects of surface texture in reciprocating contacts–an experimental study', *Tribology International*, vol. 82, pp. 28–42, 2015, https://doi.org/10.1016/j.triboint.2014.09.015

[41] A. Razumić, B. Runje, Z. Keran, Z. Trzun, and D. Pugar, 'Reproducibility of Areal Topography Parameters Obtained by Atomic Force Microscope', *Tehnički glasnik*, vol. 19, no. si1, pp. 1–6, Jun. 2025, https://doi.org/10.31803/tg-20250324183037

[42] Z. Wang, X. Rong, L. Zhao, X. Xing, and H. Ma, 'Effects of Substrate Surface Characteristics on the Adhesion Properties of Geopolymer Coatings', *ACS Omega*, vol. 7, no. 14, pp. 11988–11994, Apr. 2022, https://doi.org/10.1021/acsomega.2c00170

[43] J. P. B. Van Dam, S. T. Abrahami, A. Yilmaz, Y. Gonzalez-Garcia, H. Terryn, and J. M. C. Mol, 'Effect of surface roughness and chemistry on the adhesion and durability of a steel-epoxy adhesive interface', *International Journal of Adhesion and Adhesives*, vol. 96, p. 102450, 2020, https://doi.org/10.1016/j.ijadhadh.2019.102450

[44] B. He, S. Ding, and Z. Shi, 'A comparison between profile and areal surface roughness parameters', *Metrology and Measurement Systems*, vol. 28, no. 3, pp. 413–438, 2021, https://doi.org/10.24425/mms.2021.137133

[45] C. Moreau, J. Lemesle, D. Páez Margarit, F. Blateyron, and M. Bigerelle, 'A Statistical Approach for Characterizing the Behaviour of Roughness Parameters Measured by a Multi-Physics Instrument on Ground Surface Topographies: Four Novel Indicators.', *Metrology*, vol. 4, no. 4, 2024, https://doi.org/10.3390/metrology4040039

[46] A. Razumić, A. Horvatić Novak, B. Štrbac, V. Alar, and B. Runje, 'The influence of filtering on surface topography parameters obtained by the AFM', in *21th International Conference on Materials, Tribology & Recycling: MATRIB 2021*, 2021, pp. 418–431.

[47] R. Reizer and P. Pawlus, '3D surface topography of cylinder liner forecasting during plateau honing process', *J. Phys.: Conf. Ser.*, vol. 311, p. 012021, Aug. 2011, https://doi.org/10.1088/1742-6596/311/1/012021

[48] Y. Wang and Y. Liu, 'Preparation of measured engineering surfaces for modeling tribological systems, part I: Characterization and reconstruction', *Tribology International*, vol. 199, p. 110026, Nov. 2024, https://doi.org/10.1016/j.triboint.2024.110026

[49] D. K. Prajapati and M. Tiwari, 'Assessment of Topography Parameters During Running-In and Subsequent Rolling Contact Fatigue Tests', *Journal of Tribology*, vol. 141, no. 5, Mar. 2019, https://doi.org/10.1115/1.4042676

[50] Z. Keran, I. Stojanović, A. Horvatić Novak, B. Runje, A. Razumić, and D. Vidović, 'Corrosion Resistance of Open Die Forged Austenitic Stainless Steel Samples Prepared with Different Surfaces', *Sustainability*, vol. 13, no. 11, p. 5871, 2021, https://doi.org/10.3390/su13115871

[51] A. Razumić, L. Turkalj, A. H. Novak, I. Stojanović, and B. Runje, 'Influence of the mild steel coating application process, drying method and pigment on the surface topography', *Materials Testing*, vol. 64, no. 12, pp. 1773–1781, Dec. 2022, https://doi.org/10.1515/mt-2022-0150

https://doi.org/10.64486/m.65.1.2

[52] '3D S Hybrid Parameters – Michigan Metrology'. Accessed: May 30, 2022. [Online]. Available: https://www.michmet.com/3d_s_hybrid_parameters.htm

[53] J. Berglund, C. A. Brown, B.-G. Rosén, and N. Bay, 'Milled die steel surface roughness correlation with steel sheet friction', *CIRP Annals*, vol. 59, no. 1, pp. 577–580, Jan. 2010, https://doi.org/10.1016/j.cirp.2010.03.140

[54] P. Pawlus, R. Reizer, and M. Wieczorowski, 'Parametric characterization of machined textured surfaces', *Materials*, vol. 16, no. 1, p. 163, 2022, https://doi.org/10.3390/ma16010163

[55] P. Pawlus and R. Reizer, 'Functional importance of honed cylinder liner surface texture: A review', *Tribology International*, vol. 167, p. 107409, 2022, https://doi.org/10.1016/j.triboint.2021.107409

[56] P. Podulka, 'Suppression of the high-frequency errors in surface topography measurements based on comparison of various spline filtering methods', *Materials*, vol. 14, no. 17, p. 5096, 2021, https://doi.org/10.3390/ma14175096

[57] V. Molnar, 'Experimental investigation of tribology-related topography parameters of hard-turned and Ground 16MnCr5 Surfaces', *Lubricants*, vol. 11, no. 6, p. 263, 2023, https://doi.org/10.3390/lubricants11060263

[58] D. Hüser, J. Hüser, S. Rief, J. Seewig, and P. Thomsen-Schmidt, 'Procedure to approximately estimate the uncertainty of material ratio parameters due to inhomogeneity of surface roughness', *Measurement Science and Technology*, vol. 27, no. 8, p. 085005, 2016, https://doi.org/10.1088/0957-0233/27/8/085005

[59] '3D Functional Parameters – Michigan Metrology'. Accessed: May 30, 2022. [Online]. Available: https://www.michmet.com/3d_s_functional_parameters.htm

[60] ISO 25178-3:2012 Geometrical product specifications (GPS) — Surface texture: Areal — Part 3: Specification operators.

[61] Y. Shao, Y. Yin, S. Du, T. Xia, and L. Xi, 'Leakage Monitoring in Static Sealing Interface Based on Three Dimensional Surface Topography Indicator', *Journal of Manufacturing Science and Engineering*, vol. 140, no. 101003, Jul. 2018, https://doi.org/10.1115/1.4040620

[62] M. Bourebia, S. Meddah, L. Samia, S. Achouri, A. Oulabbas, and L. Laouar, 'Study of the Influence of Volume Parameters on the Paint Coating Adhesion', in *Recent Advances in Environmental Science from the Euro-Mediterranean and Surrounding Regions (4th Edition)*, in Advances in Science, Technology & Innovation. , Cham: Springer Nature Switzerland, 2024, pp. 61–65. https://doi.org/10.1007/978-3-031-51904-8_14

[63] R. Shi, B. Wang, Z. Yan, Z. Wang, and L. Dong, 'Effect of surface topography parameters on friction and wear of random rough surface', *Materials*, vol. 12, no. 17, p. 2762, 2019, https://doi.org/10.3390/ma12172762

[64] 'Variability of areal surface topography parameters due to the change in surface orientation to measurement direction', https://doi.org/10.1002/sca.21115

[65] '3D Spatial Parameters – Michigan Metrology'. Accessed: May 30, 2022. [Online]. Available: https://www.michmet.com/3d_s_spatial_parameters.htm

[66] R. A. Waikar and Y. B. Guo, 'A comprehensive characterization of 3D surface topography induced by hard turning versus grinding', *Journal of Materials Processing Technology*, vol. 197, no. 1, pp. 189–199, Feb. 2008, https://doi.org/10.1016/j.jmatprotec.2007.05.054

https://doi.org/10.64486/m.65.1.2